IOPscience iopscience.iop.org

Home Search Collections Journals About Contact us My IOPscience

Hydrostatic limits of 11 pressure transmitting media

This article has been downloaded from IOPscience. Please scroll down to see the full text article.

2009 J. Phys. D: Appl. Phys. 42 075413

(http://iopscience.iop.org/0022-3727/42/7/075413)

View the table of contents for this issue, or go to the journal homepage for more

Download details:
IP Address: 128.112.21.237
The article was downloaded on 22/07/2011 at 20:39

Please note that terms and conditions apply.

IOP PUBLISHING JOURNAL OF PHYSICS D: APPLIED PHYSICS

J. Phys. D: Appl. Phys. **42** (2009) 075413 (7pp) doi:10.1088/0022-3727/42/7/075413

Hydrostatic limits of 11 pressure transmitting media

S Klotz, J-C Chervin, P Munsch, and G Le Marchand

IMPMC, Université P&M Curie, 140 Rue Lourmel, 75015 Paris, France

E-mail: Stefan.Klotz@impmc.jussieu.fr

Received 23 December 2008, in final form 10 February 2009
Published 13 March 2009
Online at stacks.iop.org/JPhysD/42/075413

Abstract

We present a systematic and comparative study of the pressure-induced solidification of 11 frequently used pressure transmitting fluids using the ruby fluorescence technique in a diamond anvil cell. These fluids are 1 : 1 and 5 : 1 iso-n pentane, 4 : 1 deuterated methanol–ethanol, 16 : 3 : 1 deuterated methanol–ethanol-water, 1 : 1 FC84-FC87 Fluorinert, Daphne 7474, silicone oil, as well as nitrogen, neon, argon and helium. The data provide practical guidelines for the use of these fluids in high pressure experiments up to 50 GPa.

(Some figures in this article are in colour only in the electronic version)

1. Introduction

The vast majority of high pressure experiments are aimed to be carried out under hydrostatic conditions. The reason is that hydrostatic pressure is a thermodynamic parameter and the results obtained under such conditions are intrinsic material properties which can be compared with theory. The practical realization consists of immersing the sample in a 'pressure transmitting fluid' which is supposed to support no shear. Unfortunately, the melting line of fluids eventually increases under pressure and solidification inevitably occurs at some pressure. Beyond this point, the pressure across the experimental volume is generally inhomogeneous and differential (mostly uni-axial) stress and shear stresses appear. Depending on the type of measurement, this leads to a more or less dramatic decrease in the quality and accuracy of the data and often to the appearance of 'anomalies' which might be wrongly ascribed to new physical phenomena, see Takemura *et al* [1, 2, 3] for a few illustrative examples. As high pressure techniques become more sophisticated the need for high quality data and hence for hydrostatic pressure transmitting fluids becomes more urgent. It is hence important to characterize the various fluids which are currently used in high pressure experiments, and there is indeed considerable literature on this issue. But unfortunately it is often difficult to compare these results since the experiments were carried out by different groups probing non-hydrostaticity by different techniques having widely different sensitivities, such as ruby fluorescence, x-ray diffraction, Raman line-shape, and strain measurements, and using different types of high pressure cells. In this paper we present a systematic study of various fluids which are currently used in high pressure experiments up to the Mbar range. The data are interesting since they were obtained by exactly the same procedure which allows a direct comparison between different media. The data provide solidification/glass transition pressures, as well as absolute values of pressure gradients across the sample chamber once the medium is solid. The data are useful for investigations in the 10 GPa range which include applications in large-volume devices. All experiments were carried out at ambient temperature, except in the case of Daphne 7474 where data were also taken at 50 and 100 °C.

2. Experimental

We use a diamond anvil cell (DAC) and the ruby fluorescence method as originally applied by Piermarini *et al* [4]. A recent overview of the properties of ruby under pressure and its use as a pressure sensor has been given by Syassen [5]. In most of the cases, the fluids were loaded into a membrane DAC [6] with anvil culets of 400 μm diameter and stainless steel gaskets with a 150–200 μm bore, preindented to a thickness of 40 μm. In the case of helium the culet size was 150 μm, and the gasket had a bore of 80 μm and an initial thickness of 15 μm. The medium of interest was loaded into the cell (in the case of N_2, Ar, He, Ne at 300 K and 0.1–0.2 GPa using a gas-loader [7]) after placing 5–10 ruby spheres of 3–5 μm diameter equally distributed across the bore (figure 1). Such ruby spheres were described previously [8] and are now frequently applied in high pressure experiments. Compared with the

 © 2009 IOP Publishing Ltd Printed in the UK

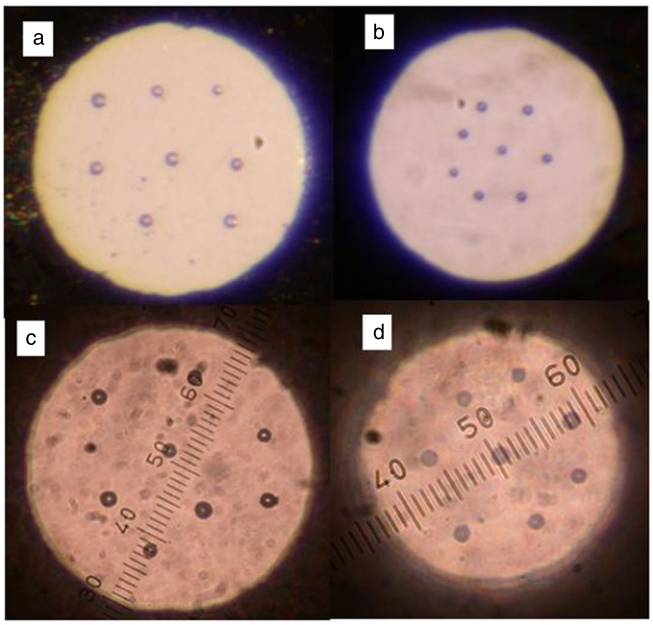

Figure 1. Pictures of DAC loaded with ruby spheres immersed in various pressure transmitting media: (*a*) 1 : 1 FC84-FC87 Fluorinert, (*b*) helium, (*c*) nitrogen, (*d*) Daphne 7474. Scales in (*c*) and (*d*): 1 division = 5 μm.

formerly used ruby 'chips' they have the advantage of being easily identifiable. The particular annealing procedure [8] ensures small fluorescence line widths which depend only little on the sphere. Ruby fluorescence was excited using an argon–ion laser (514.5 nm) and detected by a DILOR XY triple-monochromator with a focal length of 500 mm and a CCD detector cooled by liquid nitrogen. From numerous similar experiments we know that at 300 K the effect of laser radiation has no detectable influence on the temperature of the illuminated ruby. The positions of the R1 and R2 lines as well as the corresponding widths were determined by a fit using the associated LabSpec software. Pressures were obtained from the standard ruby calibration [9]. The statistical precision on the position is $\pm 0.1\,\mathrm{cm}^{-1}$ corresponding to ± 0.015 GPa. As will be shown further below, an extremely sensitive criterion for solidification is the standard deviation of the pressures P_i indicated by the N ruby spheres:

$$\sigma = \sqrt{\frac{1}{N}\sum_{i=1}^{N}(P_i - \bar{P})^2}, \qquad (1)$$

where $\bar{P}$ is the average pressure $\bar{P} = \frac{1}{N}\sum_{i=1}^{N} P_i$. For purely hydrostatic pressures $\sigma = 0$ since all ruby spheres strictly indicate the same pressure, after subtracting small but detectable offsets determined at the lowest pressure, i.e. at ~0.01 GPa. A similar analysis was first applied by Bell and Mao [10]. We found that this criterion is much more sensitive and reliable to indicate solidification and pressure gradients than the often used width $\Delta\Gamma$ of the R1 line or the R1–R2 splitting. It will be shown that in several cases we observe only a smooth variation of $\Delta\Gamma$ and R1–R2 across the solidification pressure, and which often depends strongly on the individual ruby. In contrast, the increase in σ upon solidification is very sharp and easy to define, and σ is a direct measure of the pressure inhomogeneity across the pressure chamber, once the fluid has solidified. Nevertheless, in the following we give for each medium also *average* values of $\Delta\Gamma$ and R1–R2. It should be noted, however, that in each loading we observed at least one ruby which did not follow the average trend, at elevated temperatures. This is probably due to the particular orientation of these rubies with respect to the direction of the deviatoric stress, as discussed by Syassen [5] and references therein.

3. Results

3.1. Iso-n-pentane mixtures

Figure 2 shows data on 1 : 1 iso-n-pentane which served as a test case for the method since the results can be compared with the original measurements of Piermarini *et al* [4]. The onset of detectable pressure gradients (± 0.01 kbar) is easily seen at 7.4 GPa, in good agreement with the data from [4]. These values are compared with measurements of a 5 : 1 iso-n pentane mixture, which at low temperature and moderate pressure is definitely superior to the 1 : 1 mixture [11]. Figure 2 shows that at 300 K, the difference in the solidification pressure is within error identical to the one found for the 1 : 1 mixture. The insets show in each case the pressure dependence of the fitted R1 line width and the R1–R2 splitting, which exhibit sharp kinks at the same pressure where σ increases. Pressure gradients are 10% at 15 GPa which is considerable compared with most of the other compounds studied.

3.2. Methanol–ethanol mixtures

4 : 1 methanol–ethanol is the most commonly used pressure transmitting medium and has been investigated by numerous groups which conclusively show that the glass transition is at 10.5 GPa. Traditionally this mixture is used for DAC experiments, but recently it has gained considerable importance for high pressure neutron scattering to 10 GPa [12, 13]. Neutron experiments require the use of deuterated methanol and ethanol, since hydrogen-containing material produces a strong background due to the large incoherent cross section of hydrogen. Although a significant difference compared with hydrogenated mixtures is not expected, it has never been experimentally demonstrated. The aim of our measurements was hence to investigate the effect of deuteration, but also to look at the effect of addition of water in 16 : 3 : 1 methanol–ethanol–water mixtures, which has been suggested to have a glass transition 4 GPa higher than the pure 4 : 1 fluid, i.e. at 14.4 GPa [14]. Figure 3 presents the results for the 4 : 1 and 16 : 3 : 1 fully deuterated mixtures. We find 10.5 ± 0.5 GPa in both cases. This proves that not only is the effect of deuteration negligible but also the addition of water has no detectable influence on the hydrostatic pressure range. Our results are supported by data by Angel *et al* [15] using gigaherz ultrasonics which find, at least at this frequency, the appearance of shear waves and hence solidification at 10.5 GPa.

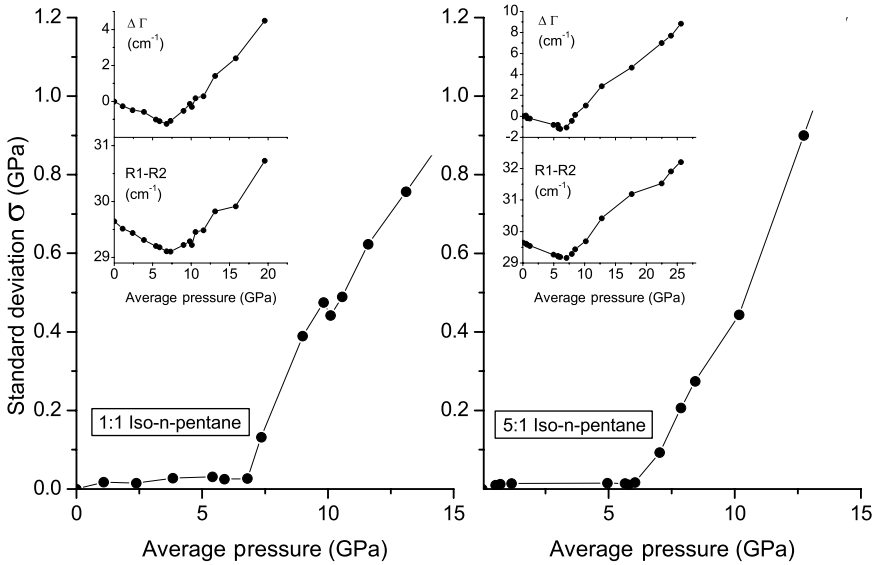

Figure 2. Pressure dependence of the standard deviation σ (main figures), the average change in R1 line width $\Delta\Gamma$ and average R1–R2 splitting (insets) for 1 : 1 iso-n-pentane (left panel) and 5 : 1 iso-n-pentane (right panel).

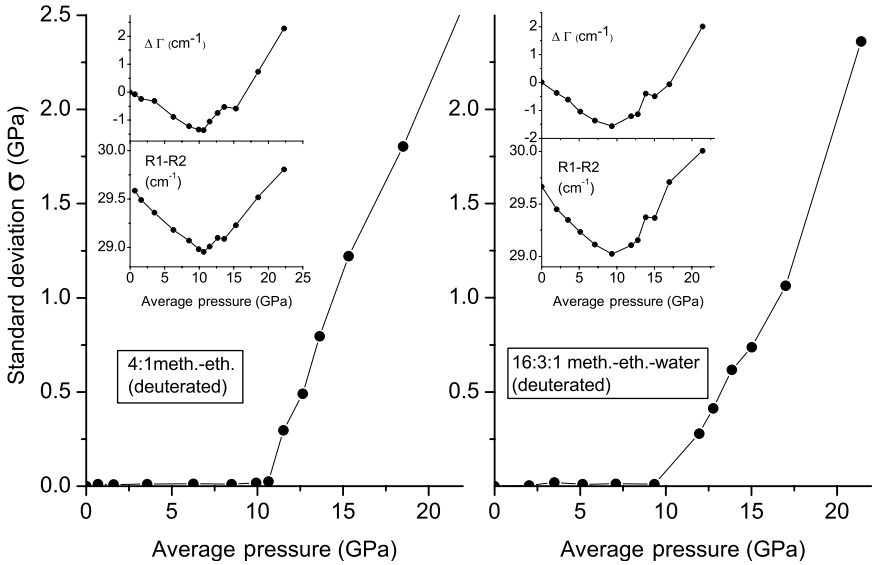

Figure 3. Pressure dependence of the standard deviation σ (main figures), the average change in R1 line width $\Delta\Gamma$ and the average R1–R2 splitting (insets) for 4 : 1 deuterated methanol–ethanol (left panel) and 16 : 3 : 1 deuterated methanol–ethanol-water (right panel).

3.3. Silicone oil

'Silicone oil' denotes a wide range of fluids based on polymerized siloxanes, in the simplest and most common case polydimethyl-siloxane with the general formula $(H_3C)[SiO(CH_3)_2]_nSi(CH_3)$. There have been at least two investigations on the visco-elastic properties of these compounds under pressure using the ruby fluorescence technique [16, 17]. Ragan *et al* [16] reported measurements on the Dow Corning 200 fluid (a polydimethyl-siloxane with a viscosity of 978 Pa s at 25 °C) and concluded from the measured R1 line width and the R1–R2 separation that the visco-elastic behaviour of this fluid is very similar to the standard 4 : 1 ethanol–methanol mixture. A more recent work by Shen *et al* [17] using the same technique up to 60 GPa and a 1 mPa s (25 °C) silicone fluid from Alfa Asear seems to confirm this and indicates that beyond 20 GPa silicone oil is in fact superior to the 4 : 1 alcohol mixture. The precision of the line width was however in both measurements only $\sim$1 cm^{-1} which compromises the conclusions drawn below 10 GPa, where the R1 line width of silicone oils was identical to the alcohol mixtures within error of the measurements. Here we use a polydimethyl-siloxane oil of type 'Rhodorsil 47V1000' commercialized by VCR with a viscosity of 0.97 Pa s at 25 °C. The inset of figure 4 indeed shows that the increase in the R1 line width remains below 1 cm^{-1} up to 8 GPa, and reaches $\sim$10 cm^{-1} at 20 GPa, which is in reasonable agreement with the previous data [16, 17]. However, the $\sigma(P)$ plot (main figure) shows that pressure differences appear already at 3 GPa and increase with pressure up to 6 GPa where gradients are typically 0.4 GPa, i.e. 7%. Surprisingly, these gradients decrease as the average pressure increases and reach a very

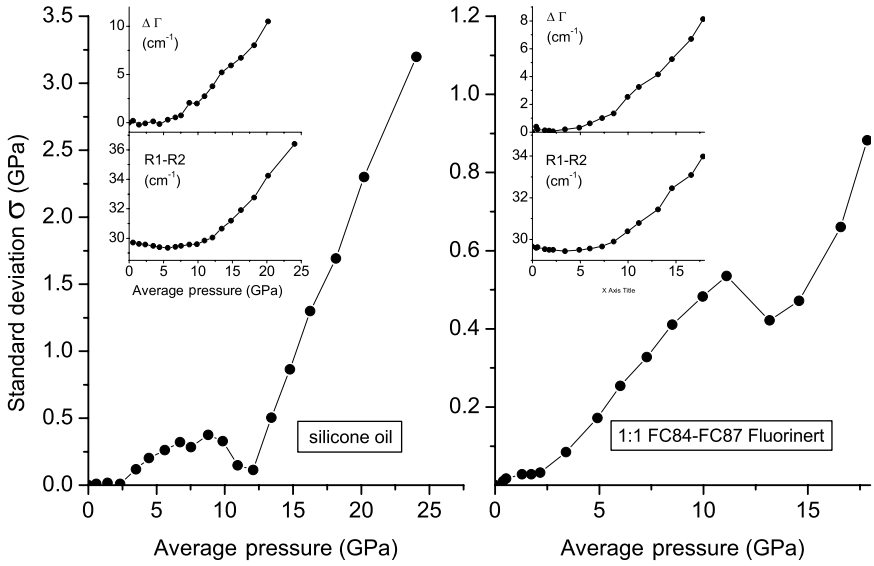

Figure 4. Pressure dependence of the standard deviation σ (main figures), the average change in R1 line width $\Delta\Gamma$ and the average R1–R2 splitting (insets) for silicone oil (left panel) and 1 : 1 FC84-FC87 Fluorinert (right panel).

low value of 1–2 kbar at 12 GPa. Upon further increase in pressure, the standard deviation increases rapidly and reaches more than 3 GPa at an average pressure of 23 GPa. We believe that the anomalous behaviour seen in figure 4 at 12 GPa is inherent to silicone oil since it appears exactly at the pressure where a phase transition was detected in the same fluid by infrared absorption [6]. It is well known that pressure gradients are reduced when structural phase transitions occur. Our data therefore show that the widespread belief that silicone oil is performing like the 4 : 1 ethanol–methanol mixture is incorrect, at least for pressures below 12 GPa.

3.4. 1 : 1 FC84-FC87 Fluorinert

Fluorinert is a trademark for a series of perfluoro-carbon liquids commercialized by 3M. Fluorinert liquids have been applied for a long time as pressure transmitting media for neutron scattering [18] since they contain no hydrogen, which would produce a large background due to the incoherent cross section of hydrogen. The most popular types for this purpose have been FC75 and FC77 with generic chemical compositions $(C_8F_{18})_n(C_8F_{16}O)_m$. It had been realized soon that the hydrostatic pressure range is very limited, up to approximately 2 GPa. Recently it has been proposed that a mixture of 1 : 1 FC84 and FC87 has superior properties [19]. Figure 4 shows that the hydrostatic pressure range extends to 2.3 GPa at most, in good agreement with the conclusions of [19]. Beyond, the pressure gradients increase rapidly and reach 0.5 GPa at 10 GPa. The inset shows that the solidification point is difficult to detect by observing the pressure dependence of the R1 line.

3.5. Daphne 7474

Daphne 7474 is a pressure transmitting fluid composed of mainly 2,2,8,8 tetra-alkylsilane and silicone oil and is commercialized by Idemitsu Kosan Corporation, Japan.

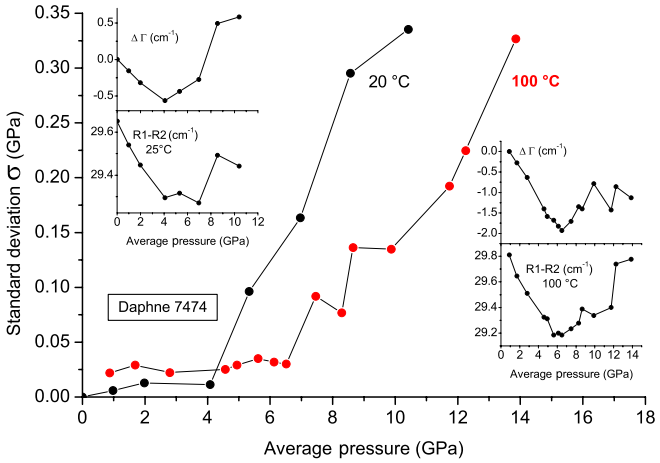

Figure 5. Pressure dependence of the standard deviation σ (main figures), average change in R1 line width $\Delta\Gamma$ and the average R1–R2 splitting (insets) for Daphne 7474 at 20 °C and 100 °C.

Similar to its related compound Daphne 7373 [20], it has become popular for magnetic measurements in clamp-type pressure cells in the GPa range for low temperature applications. At room temperature it has a density of 0.81 g cm^{-3} and a viscosity of 3.56 mPa s. We have investigated Daphne 7474 at 20, 50 and 100 °C; the essential conclusions are already published in [21]. Figure 5 shows that at 20 °C there are no detectable pressure gradients up to 3.7 GPa and at 100° up to 6.5 GPa. The solidification line can be described as $P_s(T) = 0.033T + 3.18$ (with P in GPa and T in °C), i.e. the hydrostatic pressure range can easily be doubled by modest heating.

3.6. Argon

Among the rare gases argon has the advantage that it is relatively easy to load and inexpensive. The disadvantage is its low solidification pressure, i.e. 1.4 GPa at 300 K. Bell

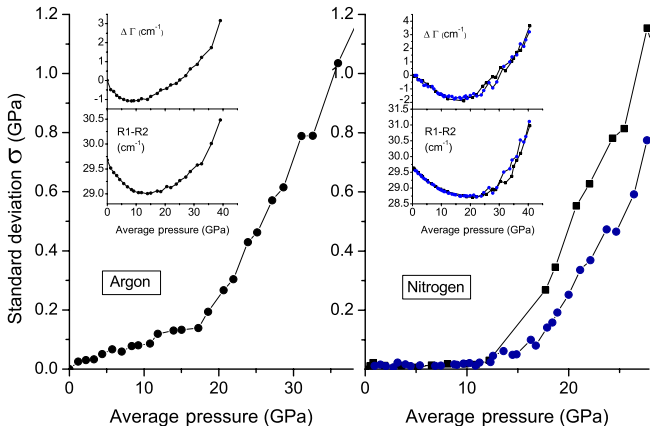

Figure 6. Pressure dependence of the standard deviation σ (main figures), the average change in R1 line width $\Delta\Gamma$ and the average R1–R2 splitting (insets) for argon (left panel) and nitrogen (right panel). For nitrogen, measurements on two loadings were carried out (squares and dots).

and Mao [10] quote a hydrostatic limit of ∼9 GPa using the ruby fluorescence method, whereas a recent work by Angel *et al* [15] claims a value slightly above the crystallization pressure, i.e. 1.9 GPa, using the broadening of the (1 0 1) single crystal Bragg reflection of quartz as an indicator. Figure 6 clarifies the considerable difference in the two measurements. Using the standard deviation as defined in (1) we detect the first signs of pressure gradients at 2 GPa, a value in rather good agreement with Angel *et al*s observations [15]. The gradients continuously increase with pressure, reach 0.1 GPa at 10 GPa (1%) and seem to increase more rapidly above ∼20 GPa. This explains the discrepancy between the reported measurements mentioned above and demonstrates how the observation of the R1 line width or R1–R2 splitting can be misleading in defining the solidification pressure. The R1 line width decreases continuously up to ∼8 GPa where it shows a shallow minimum followed by an increase to 3 cm^{-1} at 40 GPa. This indicator would hence suggest a hydrostatic limit of ∼10 GPa despite the presence of measurable pressure differences in the experimental volume. The R1–R2 splitting shows a minimum at an even higher pressure, i.e. at approximately 12 GPa.

3.7. Nitrogen

Nitrogen as pressure medium was investigated by LeSar *et al* [22] who quotes a hydrostatic limit of 13 GPa. As in the case of argon, this value is considerably higher than that quoted by Angel *et al* [15] using single crystal x-ray diffraction, i.e. 2.4 GPa. We carried out measurements on two loadings. The first measurement (figure 6, squares) showed that the R1 line width decreases up to 15 GPa and that first pressure gradients (±0.02 GPa) appear slightly above 10 GPa, which is considerably higher than Angel's value. This observation is puzzling since the sensitivity of our method is very high, i.e. pressure gradients of ±0.015 GPa (150 bar) would be detected. For this reason the experiment was repeated one year later on a second loading (figure 6, dots) which gave essentially the same results. For pressures beyond 10 GPa, the gradients rapidly increase and reach 0.6–0.8 GPa at an average pressure of 25 GPa, i.e. 3–4%. The behaviour of the R1 line width as well as the R1–R2 splitting resembles very much the observations made for argon (see figure 6), i.e. both show a shallow minimum at pressures far beyond the pressure where first pressure gradients are visible.

3.8. Neon

Neon crystallizes at 300 K at 4.8 GPa, and hence one expects that it provides better hydrostatic conditions than argon and nitrogen which solidify at 1.5 GPa and 2.4 GPa, respectively. Figure 7 confirms this, showing that the first signs of non-hydrostaticity appear at 15 GPa, which is consistent with the indications given by the R1 line width (inset) and an earlier work by Meng *et al* [23] and Bell and Mao [10]. Even beyond, the values of pressure gradients remain very small: at 50 GPa, the standard deviation of pressure detected by the different ruby spheres is less than 0.5 GPa, i.e. less than 1%. The behaviour of the R1–R2 splitting is interesting: its pressure dependence is strictly monotonic and hence very similar to the case of helium, as shown in the following section.

3.9. Helium

Helium is unquestionably the best available pressure transmitting medium, even in its solid state, i.e. above 12.1 GPa at 300 K. The recent gain in interest in its visocelastic properties up to the Mbar range is explained by the need for high-accuracy equations-of-state of simple solids (mainly elemental metals) to improve the available pressure scale. The indicators for the occurrence of non-hydrostatic conditions were mostly subtle deviations from the expected EOS, but also changes in the ruby luminescence spectra. Takemura and Dewaele [3] as well as Dewaele and Loubeyre [24] determined the R1–R2 splitting up to 150 GPa and found a linear increase, at least at pressures beyond 40 GPa [3] confirming an earlier work by Takemura [25]. This correlates with a decrease in the R1 line width up to this pressure, beyond which it was found to be essentially pressure independent [3, 24, 25]. These data compare very well with our own observations, shown in figure 7. The R1 line width decreases monotonically to ∼25 GPa and then increases slightly beyond. At the same time the standard deviation of the pressures indicated by the six ruby spheres remains flat up to ∼23 GPa where it starts to increase under pressure to reach 0.15 GPa at 40 GPa, i.e. 0.4%. This value can be compared with the one found in neon at the same pressure, i.e. 0.3 GPa. We note, however, that the sigma values for He might be underestimated compared with the measurements on the other fluids since the gasket hole was smaller and hence the ruby spheres were closer to each other.

4. Discussion and conclusion

This paper presents a refined method to detect pressure gradients in DACs. Compared with other methods it has the advantage that it can be readily carried out in any laboratory to characterize the visco-elastic behaviour of pressure transmitting media at variable temperature, while

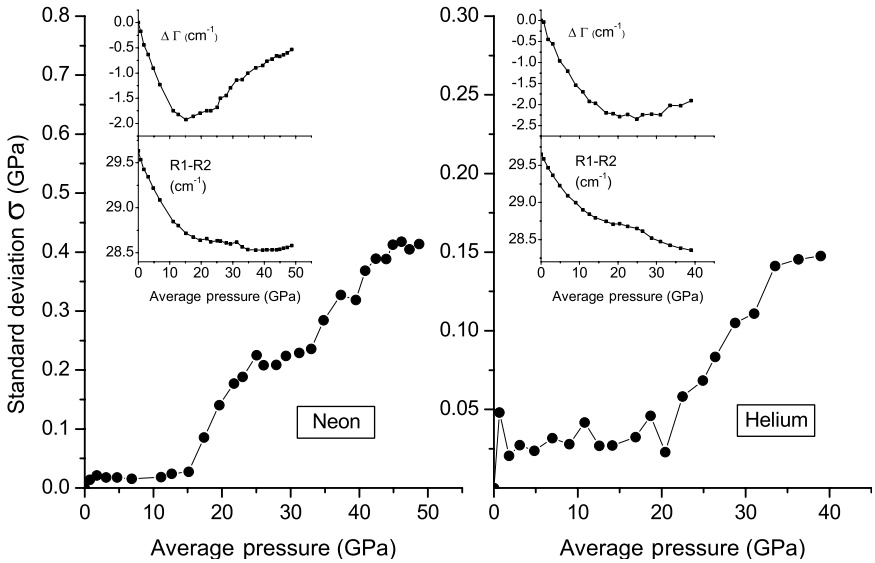

Figure 7. Pressure dependence of the standard deviation σ (main figures), the average change in R1 line width $\Delta\Gamma$ and the average R1–R2 splitting (insets) for neon (left panel) and helium (right panel).

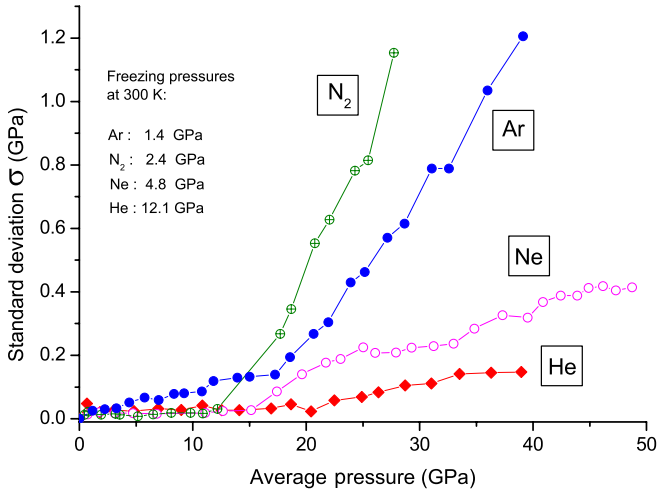

Figure 8. Comparison of pressure dependences of the standard deviation σ of N_2, Ar, Ne and He. The inset gives freezing pressures at 300 K cited in [26, 27, 28, 29] for Ar, N_2, Ne and He, respectively.

attaining a sensitivity comparable to indicators based on single crystal diffraction. The measurements demonstrate the shortcomings of making claims on hydrostaticity based on the measurement of the R1 line width $\Delta\Gamma$ or the R1–R2 splitting on a single ruby in the DAC. For the pentane and alcohol mixtures as well as Daphne 7474 (figures 2, 3 and 5), the solidification pressures indicated by the minima in $\Delta\Gamma$ and R1–R2 are more or less identical. This is not the case for the other fluids where R1–R2 systematically indicates a considerably higher solidification pressure (figures 4, 6 and 7). In the case of helium, no minimum of R1–R2 could be detected at all up to 40 GPa, though it would appear at higher pressures [2, 3, 24]. The general conclusion is that, if there is only one single ruby available, the R1-width appears to be a more reliable indicator for non-hydrostaticity.

Overall, our data confirm the more recent findings based on x-ray diffraction indicators and quantify the degree of non-hydrostaticity occurring in these media under pressure [3, 15, 24]. The comparison between solidified gases in the 0–10 GPa range is particularly interesting (figure 8). As expected, argon ranks at the lower end and helium at the top. But we find that in the 0–10 GPa range nitrogen can compete with neon, despite its lower solidification pressure, i.e. 2.4 GPa compared with 4.8 GPa. As mentioned further above, the observation that we cannot detect significant pressure inhomogeneities in nitrogen in the 0–10 GPa range seems to contradict the results from single crystal diffraction [15] but was clearly confirmed in a second loading. This suggests that up to 10 GPa nitrogen could be a very suitable alternative to neon which is costly and more difficult to load. The measurements on nitrogen also give important information on the reproducibility of the measurements. The orientation, distribution and size of the ruby spheres in the pressure cell are more or less random; nevertheless, the result of the two measurements are remarkably consistent (figure 6). Concerning the alcohol mixtures, our data clearly show that the addition of water to the 4 : 1 methanol–methanol mixture has only a marginal effect on the range of hydrostaticity, if at all.

It should be noted that the requirement on hydrostaticity depends considerably on the type of measurement and the sample under investigation. A useful number for the maximum tolerable pressure gradient in a measurement of the physical property x with a technique of resolution ϵ is $\Delta P < B\epsilon/\gamma$, where $\gamma = -\partial \ln x/\partial \ln V$ is the 'Grüneisen parameter' of x and B the bulk modulus of the sample. This is because a difference in pressure ΔP in the pressure chamber will entail a difference in the physical property x of $\Delta x = x\gamma\Delta P/B$, which cannot be detected if $\Delta x/x$ is smaller than the resolution ϵ. The obvious difficulty is that this estimation requires prior knowledge of the quantity sought, i.e. the pressure dependence of x. But since γ is frequently of the order of 1, the above estimate reduces to $\Delta P < B\epsilon$. To give an example, the resolution in determining lattice parameters in

high pressure synchrotron powder diffraction is approximately 10^{-3}. The maximal tolerable pressure gradient in a diffraction measurement (x is in this case the d-spacings of the Bragg reflections) on a solid with a bulk modulus of 100 GPa is hence in the order of 0.1 GPa. Using helium as a pressure transmitting medium, such gradients will have accumulated at ∼30 GPa according to figure 8. This is indeed consistent with what is reported in [3].

Acknowledgments

The authors are grateful to Professor K Murata (Osaka City University) and Jean-Luc Laborier (Institut Laue-Langevin, Grenoble) for providing samples of Daphne 7474 and Fluorinert, respectively. A part of the measurements were carried out by Amine Firar and Amélie Adet. The authors acknowledge helpful discussions with K Takemura and the aid of Thalia Klotz in the preparation of the manuscript. The manuscript was improved following the comments of two anonymous referees.

References

[1] Takemura K 2005 *Proc. Joint 20th AIRAPT and 43rd EHPRG Conf. (Karlsruhe 2005)* ISBN 3-923704-49-6
[2] Takemura K 2007 *J. Phys. Soc. Japan. Suppl.* A **76** 202
[3] Takemura K and Dewaele A 2008 *Phys. Rev.* B **78** 104119
[4] Piermarini G J, Block S and Barnett J D 1973 *J. Appl. Phys.* **44** 5377
[5] Syassen K 2008 *High Pressure Res.* **28** 75
[6] Chervin J-C, Canny B, Besson J M and Pruzan Ph 1995 *Rev. Sci. Instrum.* **66** 2595
[7] Couzinet B, Dahan N, Hamel G and Chervin J C 2003 *High Pressure Res.* **23** 409
[8] Chervin J C, Canny B and Mancinelli M 2001 *High Pressure Res.* **21** 305
[9] Mao H K, Xu J and Bell P M 1986 *J. Geophys. Res.* B **91** 4673
[10] Bell P M and Mao H K 1981 *Carnegie Institution of Washington Year Book* vol 80, pp 404–6
[11] Klotz S, Philippe J and Cochard E 2006 *J. Phys. D: Appl. Phys.* **39** 1674
[12] Marshall W G and Francis D J 2002 *J. Appl. Cryst.* **35** 122
[13] Klotz S, Strässle Th, Rousse G, Hamel G and Pomjakushin V 2005 *Appl. Phys. Lett.* **86** 031917
[14] Fujishiro I, Piermarini G J, Block S and Munro R G 1982 *Proc. 8th AIRAPT Conf. (Uppsala, 1982)* vol II, p 608
[15] Angel R J, Bujak M, Zhao J, Gatta G D and Jacobsen S D 2007 *J. Appl. Cryst.* **40** 26
[16] Ragan D D, Clark D R and Schiferl D 1996 *Rev. Sci. Instrum.* **67** 494
[17] Shen Y, Kumar R S, Pravia M and Nicol M F 2004 *Rev. Sci. Instrum.* **75** 4450
[18] McWhan D B, Birgeneau R J, Bonner W A, Taub H and Axe J D 1975 *J. Phys. C: Solid State Phys.* **8** L81
[19] Sidorov V A and Sadykov R A 2005 *J. Phys.: Condens. Matter.* **17** S3005
[20] Yokogawa K, Murata K, Yoshino H and Aoyama S 2007 *J. Phys. Soc. Japan.* **46** 3636
[21] Murata K *et al* 2008 *Rev. Sci. Instrum.* **79** 085101
[22] LeSar R, Ekberg S A, Jones L H, Mills R L, Schwalbe L A and Schiferl D 1979 *Solid State Commun.* **32** 131
[23] Meng Y, Weidner D J and Fei Y 1993 *Geophys. Res. Lett.* **20** 1147
[24] Dewaele A and Loubeyre P 2007 *High Pressure Res.* **27** 419
[25] Takemura K 2001 *J. Appl. Phys.* **87** 662
[26] Zha C S, Boehler R and Ross M 1986 *J. Chem. Phys.* **85** 1034
[27] Zinn A S, Schiferl R and Nicol M F 1987 *J. Chem. Phys.* **87** 1267
[28] Vos W L, Young D A and Ross M 1991 *J. Chem. Phys.* **94** 3835
[29] Vos W L, van Hinsberg M G E and Schouten J A 1990 *Phys. Rev.* B **42** 6106